

Dynamical Friction and The Evolution of Satellites in Virialized Halos: The Theory of Linear Response

Monica Colpi¹, Lucio Mayer¹, & Fabio Governato²

ABSTRACT

The evolution of a small satellite inside a more massive truncated isothermal spherical halo is studied using both the Theory of Linear Response for dynamical friction and N -Body simulations. The analytical approach includes the effects of the gravitational wake, of the tidal deformation and the shift of the barycenter of the primary, so unifying the local versus global interpretation of dynamical friction. The N -Body simulations followed the evolution of both rigid and live satellites within larger systems. Sizes, masses, orbital energies and eccentricities are chosen as expected in hierarchical clustering models for the formation of structures. Results from this coupled approach are applicable to a vast range of astrophysical problems, from galaxies in galaxy clusters to small satellites of individual galaxies. The main contribution to the drag results from the gravitational pull of the overdensity region trailing the satellite's path since the stellar response to the external perturbation remains correlated over a time shorter than the typical orbital period. The analytical approach and the N -Body experiments demonstrate that there is no significant circularization of the orbits and that the dynamical friction time scale is weakly dependent on the circularity ε . While the theory and the N -Body simulations give a complete description of the orbital decay of satellites a good fitting formula for the orbital decay time is:

$$\tau_{DF} = 1.2 \frac{J_{cir} r_{cir}}{[GM_{sat}/e] \ln(M_{halo}/M_{sat})} \varepsilon^{0.4}$$

where J_{cir} and r_{cir} are, respectively, the initial orbital angular momentum and the radius of the circular orbit with the same energy of the actual orbit. Tidal stripping can reduce the satellite's mass by 60% after the first pericentric passage increasing the orbital decay time. The “e” factor keeps that effect into account and should be removed in the simplified case of rigid satellites. In cosmologically relevant situations our model gives orbital decay times larger by a factor of 2 with respect to most previous estimates.

For peripheral orbits where the apocenter is larger than the virial radius of the primary decay, the global tidal field and the shift of the barycenter become important. In this case τ_{DF} needs to be further increased by at least $\simeq 50\%$. The final fate of a satellite is determined by its robustness against the effect of tides. While low density satellites are disrupted over a time comparable to the decay time of their rigid counterparts, satellites with small cores can survive up to an Hubble time within the primary, notwithstanding the initial choice of orbital parameters. Dwarf spheroidal satellites of the Milky Way, like Sagittarius A and Fornax, have already suffered mass stripping and, with their present masses, the sinking times exceed 10 Gyr even if they are on very eccentric orbits.

Subject headings: celestial mechanics, stellar dynamics – galaxies: evolution – stars: kinematics – cosmology: groups

¹Dipartimento di Fisica, Università Degli Studi di Milano, Milano, Via Celoria 16, I-20133 Milano, Italy

²Osservatorio Astronomico di Brera, Merate, via Bianchi 46, I-23807 Merate (LC) - Italy

1. Introduction

Dynamical friction is a fundamental physical process that drives the evolution of most cosmological structures, from satellites in galaxies, to galaxies in large clusters. The satellites or the galaxies can decay toward the center of the halos as friction causes the loss of orbital energy and angular momentum. This braking force is a force of back-reaction resulting from the global distortion of the stellar density field induced in the primary by the satellite’s gravity.

The theory of linear response (TLR) is an ideal tool for studying the dynamics of sinking satellites in spherical halos. Recently explored by Colpi & Pallavicini (1998, CP in the following), this formalism is alternative to other perturbative techniques developed to overcome the limits of Chandrasekhar’s theory of dynamical friction (Chandrasekhar 1943), that restricts to infinite, uniform, non selfgravitating stellar backgrounds. In TLR, the force can either be related to the density changes, or be viewed as a direct manifestation of the fluctuation-dissipation theorem (CP; Nelson & Tremaine 1997; Bekenstein & Maoz 1992; Kandrup 1981). In the last interpretation, the fluctuations of the microscopic two body force (between the satellite and the particles) add to give a nonvanishing drag. The force is the result of a time integral keeping memory of the actual dynamics of the satellite and of the dynamics of the stars as derived from their Hamiltonian. The stellar reaction to the external perturbation and the amount of dissipation that follows depend closely on the (self)-correlation properties of the underlying stellar field (Colpi 1998, C98 hereafter).

TLR has been successful in describing the decay of satellites spiraling outside their primary spherical halos, and in describing their deceleration in shortlived penetrating encounters. In the first case, global tidal deformations excited during orbital motion are responsible to the loss of stability of the satellite’s orbit (C98). In flybys (CP), the deceleration was viewed as a superposition of two effects: the gravitational pull from the overdensity region that forms just behind the satellite’s trail and the brake from extended tides.

Cosmological simulations aimed at studying the building up of cosmic structures (Ghigna et al. 1998; Tormen et al. 1998; Kravtsov & Klypin 1998) show that the majority of the satellite’s (or substructure) orbits have rather large eccentricities, and apocenters that rarely exceed twice the virial radius of the primary halo (defined as the radius where the average density inside the halo is 200 times the critical one). In this work we consider the fate of satellites placed on cosmologically relevant orbits, using TLR and N -Body simulations as a tool for exploring the decay in a self-gravitating spherical halo.

TLR is a major advance relative to alternative analytical studies (Weinberg 1986; Weinberg 1989; Séguin & Dupraz 1994) as it embraces in a relatively simple way all aspects of the gravitational interaction of the satellites with the collisionless background: the wake and the tides in a self-gravitating system, and the shift of the stellar center of mass. We then explore the dependence of the sinking times as a function of the orbital parameters and the possible role played by mass stripping on their evolution. A previous analysis was carried on by Lacey & Cole (1993) in their semi-analytical treatment of the merging of cosmic structures. The aim was to clarify the role of dynamical friction in determining the merging rate of the luminous part of galaxies as opposed to the merging rate of their dark matter halos. A dependence of the decay time on eccentricity was introduced by simply fitting the decay time curve obtained using Chandrasekhar’s formula for a point-like satellite and for a fixed orbital energy (the orbital energy was such that a circular orbit had a radius equal to the virial radius of the primary halo). The authors found that satellites on nearly-circular orbits decay on a timescale which is almost 3 times longer than that of satellites on very eccentric orbits. However satellites accreting on larger halos are usually on more tightly bound orbits according to cosmological simulations, i.e. even radial orbits have apocenters close to the virial

radius of the main halo (in the Lacey & Cole case the apocenter of radial orbits was well outside the virial radius). A more appropriate choice of the orbital parameters is thus needed to determine to what extent the sinking times depend on the eccentricity of the orbits. Moreover, dark matter halos of individual satellites would not dissolve immediately: Navarro et al. (1995), using N -Body/SPH simulations, have shown that discarding the dark matter mass can lead to an overestimate of the sinking times of the baryonic cores. It is thus evident that a complete description of the orbital evolution of satellites has to take into account the effect of tidal stripping on the decay times of satellites. It is also necessary to find out if the orbits circularize during the decay, this being another long-standing issue. If orbits do circularize, we expect the initial distribution of orbital eccentricities of the satellites to be substantially altered, and this could prolong their lifetimes in the primary halos, provided that a substantial mismatch between decay times on eccentric and circular orbits does really exist.

Recently, van den Bosch, Lewis, Lake & Stadel (1999, vBLLS hereafter) carried on a series of N -Body simulations of satellites placed inside a nonsingular tidally limited spherical halo. They did not include tidal stripping treating the satellites as rigid spheres. To study the orbital evolution of satellites in a fully self-consistent way and to complement the results obtained with TLR, we have performed a number of high resolution N -Body simulations with the parallel binary treecode PKDGRAV (Stadel & Quinn 1998; Dikaiakos & Stadel 1996; vBLLS) for both rigid and deformable satellites.

The outline of the paper is as follows: in §2 we give a brief description of the theory of linear response for dynamical friction setting the framework for the calculation carried in §3. In §4 we illustrate the results of our semianalytical study and compare them with vBLLS. In §5 we explore the self-correlation properties of the equilibrium stellar system in terms of the correlation time scale and study the fading of the density wake in a uniform infinite medium. In §6 we extend our analysis to the important case of non-rigid satellites. §7 contains our conclusions.

2. The theory of Linear Response for Dynamical Friction

A satellite bound to a primary galaxy experiences in its motion a dissipative force that results from the collective response of the background to its perturbation. In TLR, the response depends just on the properties of the underlying matter field in its unperturbed state: The (self)-correlations existing among the particles ultimately leads to energy dissipation.

Under the hypothesis that the N – stars (of mass m) or dark matter particles are in virial spherical equilibrium, the drag force \mathbf{F}_Δ on a satellite described as a point like object of mass M reads

$$\mathbf{F}_\Delta(t) = GMm \sum_{i=1}^N \int_{t_0}^t ds \int d\Gamma \left[\nabla_{\mathbf{p}_i(s)} f_0 \cdot \frac{\mathbf{R}(s) - \mathbf{r}_i(s)}{|\mathbf{R}(s) - \mathbf{r}_i(s)|^3} \right] \left[GMm \sum_j^N \frac{\mathbf{R}(t) - \mathbf{r}_j(t)}{|\mathbf{R}(t) - \mathbf{r}_j(t)|^3} \right] \quad (1)$$

where $d\Gamma$ is the elementary volume in the $6N$ dimensional phase space (Γ) of the stars in the galaxy, and f_0 the N -point equilibrium distribution function (we drop the subscript *sat* hereafter to follow closely the notation of CP and denote the total halo mass M_{halo} as Nm). The drag on M is a consequence of a memory effect that develops with time and involves a suitable phase space average of the microscopic two-body force. It requires the knowledge of the dynamics of the N stars ($\mathbf{r}_i(s), \mathbf{p}_i(s)$), as determined by

the unperturbed Hamiltonian, over the whole interaction time from t_0 (when the perturbation is turned on) to the current time t . The distribution function f_0 incorporates the properties of the system in virial equilibrium.

Dark matter halos in virial equilibrium can be regarded as an assembly of collisionless particles subject to a mean field potential Ψ_0 that can be computed solving simultaneously the Poisson and Boltzmann equation. The distribution function can thus be written in terms of the one-particle phase space density $f^{\text{op}}(\mathbf{r}, \mathbf{p})$. Under this hypothesis, and due to the statistical independence of the particles, all cross correlation terms cancel identically in the limit of $N \gg 1$. Only the self-correlation properties of the collisionless background survive to yield

$$\mathbf{F}_\Delta(t) = [GM]^2 N m^2 \int_{t_0}^t ds \int d_3\mathbf{r} d_3\mathbf{p} \left\{ \nabla_{\mathbf{p}(s)} f^{\text{op}} \cdot \left[\frac{\mathbf{R}(s) - \mathbf{r}(s)}{|\mathbf{R}(s) - \mathbf{r}(s)|^3} - \int d_3\mathbf{r}' n_0(r') \frac{\mathbf{R}(s) - \mathbf{r}'}{|\mathbf{R}(s) - \mathbf{r}'|^3} \right] \right\} \frac{\mathbf{R}(t) - \mathbf{r}(t)}{|\mathbf{R}(t) - \mathbf{r}(t)|^3} \quad (2)$$

The new term appearing in brackets (involving the equilibrium background density $n_0(r)$) represents, at a given time s , the mean force acting on M resulting from the system as a whole: It accounts for the shift of the center of mass of the galaxy during the encounter. The recoil of the halo (due to linear momentum conservation) is a coherent shift of all the orbits of the background particles, giving origin to a global correlation among them. TLR, as is formulated, can account for that shift naturally and permits use of the one-particle distribution function f^{op} for the system in virial equilibrium (see CP and C98). Thus, \mathbf{F}_Δ in the form of equation (2) is the force as measured in the non-inertial reference frame comoving with the halo's center of mass.

In the context of the fluctuation-dissipation theorem, the braking force can be seen as an integral over time of the correlation function of a fluctuating component of the microscopic force

$$F_\Delta^a(t) \equiv \int_{t_0}^t ds K^a(t-s) = \int_{t_0}^t ds \int d_3\mathbf{r} d_3\mathbf{p} \nabla_{\mathbf{p}(s)}^b f^{\text{op}} T^{ba} \quad (3)$$

where the self-correlation tensor reads

$$T^{ba} \equiv [GM]^2 N m^2 \left[\frac{R^b(s) - r^b(s)}{|\mathbf{R}(s) - \mathbf{r}(s)|^3} - \int d_3\mathbf{r}' n_0(r') \frac{R^b(s) - r'^b}{|\mathbf{R}(s) - \mathbf{r}'|^3} \right] \frac{R^a(t) - r^a(t)}{|\mathbf{R}(t) - \mathbf{r}(t)|^3}. \quad (4)$$

The correlation function $K^a(t-s)$ introduces a time scale τ^* characterizing the rise time of the force $F_\Delta^a(t)$: It is the scale over which the stars redistribute the satellite's orbital energy into the internal degrees of freedom of the system.

The interpretation of \mathbf{F}_Δ in terms of a global time dependent density deformation is possible also within TLR, noting that equation (2) can be written formally as

$$\mathbf{F}_\Delta = -GMNm \int d_3\mathbf{r} \Delta n(\mathbf{r}, t) \frac{\mathbf{R}(t) - \mathbf{r}}{|\mathbf{R}(t) - \mathbf{r}|^3} \quad (5)$$

where the function $\Delta n(\mathbf{r}, t)$ maps the response, i.e., the time dependent changes in the density field $n_0(r) + \Delta n(\mathbf{r}, t)$ resulting from the superposition (memory) of disturbances created by the satellite over the entire evolution; the function $\Delta n(\mathbf{r}, t)$ can be derived comparing equation (5) with (2) (see also CP for details).

Equation (2) applies when the interaction potential between M and the stars is weak relative to the mean field potential Ψ_0 of the equilibrium system (when in isolation). This is the reason why only the properties of the halo in virial equilibrium are requested to evaluate \mathbf{F}_Δ . As a consequence of that \mathbf{F}_Δ is accurate to second order in the coupling constant G . Higher orders terms would describe the self-gravity of the response, i.e., the modification in the self interaction potential due to the external perturbation driven by M . Equation (2) can describe the sinking of satellites moving on arbitrary orbits, even outside the primary halo. Previous semianalytical studies focussed on purely circular orbits (Weinberg 1986) to explore the role of resonances and on almost radial orbits to explore the transient nature of the interaction (Séguin & Dupraz 1994).

3. TLR: the Force of Back-reaction in a Spherically Symmetric Galactic Halo

In a nonuniform collisionless background the back-reaction force on M results, in the high speed limit, from the combined action of a global tidal response related to the density gradients (absent in an infinite uniform medium) and from the development of an extended wake forming behind the satellite's path that contributes mostly to its deceleration. The force acquires a component along \mathbf{R} as symmetry around \mathbf{V} is lost, the underlying system being non homogeneous.

To estimate the drag in the domain where the satellite's velocity \mathbf{V} (determined primarily by the mean field potential Ψ_0 of the unperturbed background) maintains comparable to the background velocity dispersion, we avoid to separate out the tidal and frictional contributions being aspects of a unique process. Exploiting the time independence of the distribution function f^{op} and of the phase-space volume $d_3\mathbf{r} d_3\mathbf{v}$ (f^{op} hereafter will be considered as a function of \mathbf{r} and $\mathbf{v} = \mathbf{p}/m$ and is normalized accordingly), the drag force (eq. [2]) can be equivalently written as

$$\mathbf{F}_\Delta = [GM]^2 Nm \int_{t_0}^t ds \int d_3\mathbf{r} d_3\mathbf{v} \nabla_{\mathbf{v}} f^{\text{op}}(\mathbf{r}, \mathbf{v}) \cdot \left[\nabla_{\mathbf{R}(s)} \phi(|\mathbf{R}(s) - \mathbf{r}|) - \int d_3\mathbf{r}' n_0(r') \nabla_{\mathbf{R}(s)} \phi(|\mathbf{R}(s) - \mathbf{r}'|) \right] \nabla_{\mathbf{R}(t)} \phi(|\mathbf{R}(t) - \mathbf{r}(t-s)|) \quad (6)$$

where ϕ is proportional to the newtonian gravitational potential

$$\phi(|\mathbf{R} - \mathbf{r}|) \equiv -\frac{1}{|\mathbf{R} - \mathbf{r}|}. \quad (7)$$

In equation (6), \mathbf{R} denotes the satellite position vector relative to the halo's center of mass, and is computed self-consistently following the actual dynamics of the satellite (that now acquires the reduced mass μ).

Because of the difficulty of including the dynamics of the stars as determined by the unperturbed Hamiltonian we are led to approximate their motion as linear giving

$$\mathbf{r}(t-s) = \mathbf{r} + (t-s)\mathbf{v}. \quad (8)$$

We will compare our model with N -Body simulations (described in §4) to test indirectly the validity of such an approximation. In neglecting the acceleration of the stars, i.e., their “curvature”, during the interaction of the satellite we introduce a simplification which will prove to be satisfactory.

The shortcoming of TLR is its inability to describe short distance encounters as it is derived from a linear analysis expanded to first order in the perturbation. For a pointlike satellite moving in an infinite

uniform medium, these encounters lead to a minimum impact parameter which is determined uniquely by V and the background velocity dispersion σ . Satellites have finite size and as in N -Body simulations the short-distance two-body interaction ϕ is smoothed introducing in the microscopic gravitational potential a softening length ϵ . The necessity of a closer comparison with numerical simulations led us to consider the spline kernel potential ϕ_{sp} (Hernquist & Katz 1989) as interaction potential between the satellite and the stars reducing to the newtonian form (eq. [7]) at 2ϵ . The introduction of the softening length in the computation of the force accounts for the finite size of M permitting an unambiguous comparison with the numerical simulations by vBLLS. The drag force depends on the response of the stars and, in turn, on the characteristics of their equilibrium state which is described below.

Dark halos are often modelled as truncated non-singular isothermal spheres with a core (vBLLS; Hernquist 1993): accordingly, their density profile

$$n_0(r) = \frac{1}{2\pi^{3/2} g r_t} \frac{\exp(-r^2/r_t^2)}{(r^2 + r_c^2)} \quad (9)$$

declines exponentially at radii exceeding the tidal (or truncation) radius r_t . The homogenous core of radius r_c is surrounded by a region where $n_0(r) \propto r^{-2}$, as in a singular isothermal sphere. The constant

$$g = 1 - \pi^{1/2} \left(\frac{r_c}{r_t} \right) \exp(r_c^2/r_t^2) \left[1 - \operatorname{erf} \left(\frac{r_c}{r_t} \right) \right] \quad (10)$$

is introduced to guarantee that $\int d_3\mathbf{r} n_0(r) = 1$.

The one-dimensional background velocity dispersion σ is computed according to the second-order Jeans equation

$$\sigma^2(r) \equiv \frac{1}{n_0(r)} \int_r^\infty dr' n_0(r') \frac{4\pi G}{r'^2} \int_0^{r'} dr'' (r'')^2 n_0(r'') \quad (11)$$

and is a local function of r . For $r_c \rightarrow 0$

$$\sigma^2(r) = \frac{GNm}{g r_t} \left(\frac{r}{r_t} \right)^2 \exp(r^2/r_t^2) \int_{(r/r_t)}^\infty dx \exp(-x^2) x^{-4} \operatorname{erf}(x) \quad (12)$$

giving $\sigma^2 \simeq GNm/(g r_t \sqrt{\pi})$, at $r \ll r_t$. The back-reaction force on M is derived under the hypothesis that the one-particle distribution function is isotropic and Gaussian in the velocity space, with σ^2 computed according to equation (12):

$$f^{\text{op}}(\mathbf{r}, \mathbf{v}) = n_0(r) \left(\frac{1}{2\pi\sigma^2} \right)^{3/2} \exp(-v^2/(2\sigma^2)). \quad (13)$$

This choice is dictated not only by simplicity arguments but by the fact that collisionless systems with these characteristics are found to be nearly in equilibrium (Hernquist 1993; vBLLS) and hence are viable for describing the unperturbed system equilibrium state required by TLR. Given f^{op} , we compute \mathbf{F}_Δ from equation (6). Not all multiple integrals of equation (6) can be carried out analytically; only those over the velocity phase space are evaluated and the complex expression of the drag is reported in the Appendix.

The evolution of a satellite, of reduced mass $\mu = MNm/(M + Nm)$, is followed solving for the equations of motion, in the reference frame comoving with the center of mass of the primary halo:

$$\mu \frac{d^2 \mathbf{R}(t)}{dt^2} = -GNm \frac{\mathbf{R}(t)}{|\mathbf{R}(t)|^3} \int_{r' < R(t)} d_3\mathbf{r}' n_0(r') + \mathbf{F}_\Delta \quad (14)$$

The mass ratio M/Nm and the cusp ϵ , entering the effective potential ϕ_{sp} , are the only parameters of the model.

4. The Sinking of the Rigid Satellites

In this section we explore the evolution of satellite orbits comparing results obtained using TLR with our N -Body runs and, where possible, with those of vBLLS. As in vBLLS, the primary system, scaled to the Milky Way’s halo, is a spherical isothermal halo with a mass of $10^{12}M_{\odot}$, a tidal radius r_t of 200 kpc and a core radius $r_c = r_t/50$. In the N -Body simulations the primary halo has 10^4 particles: it was first evolved in isolation for 10 Gyr and the stability of the density profile was verified. The satellite is fifty times lighter than the primary ($M = Nm/50$). Its mass distribution is described by a rigid spline softened potential with a length scale of 3.4 kpc, comparable to the effective radius of the Large Magellanic Cloud ($\epsilon = 0.0172 r_t$). With these choices the time unit $T_0 = [GNm/r_t^3]^{(-1/2)}$ is of 1.34 Gyr.

4.1. The Dynamical Friction Decay Time and the Evolution of e for Rigid Satellites

Cosmological simulations have shown that in the hierarchical clustering scenario most of satellite’s orbits have pericenter varying between $0.2 < r_{peri}/r_t < 0.5$ and apocenter $r_{apo} < 2r_t$ (Ghigna et al. 1998). More loosely bound orbits are unlikely as their apocenter can exceed the turnaround radius (of about $2r_t$) of the major overdensity that produced the primary halo. Moreover, orbits are found to be quite eccentric on average, with a typical apocenter to pericenter distance ratio $\sim 6 - 8$ corresponding to eccentricities between 0.6 and 0.8. Below we focus attention on orbits with reference circular radii r_{cir} (determining the initial energy) in the range $0.5 \leq r_{cir}/r_t \leq 1$ (to fulfill the above inequalities). We are thus able to study the dependence of τ_{DF} both on eccentricity and orbital energy.

Figure 1 shows the dynamical evolution of the satellite set on bound orbits having initially equal energy but different eccentricity: $e = 0.8$ (top left panel), 0.6, 0.3, and 0 (lower right panel) respectively. The radius of the circular orbit at the onset of evolution is $r_{cir}/r_t = 0.5$ as in vBLLS: the selected runs coincide with models 3,4,5,6 (we refer to the table of content 1 of vBLLS). To characterize the decay and quantify the results, we report in Figure 2 the angular momentum as a function of time (in Gyr); dots are the results of the N -Body simulations carried out by vBLLS. The agreement between theory and N -Body simulations is excellent to a few %.

The analysis of more loosely bound orbits has been carried out using both TLR (for $r_{cir}/r_t = 0.8, 1$) and N -Body simulations ($r_{cir}/r_t = 1$). The results show once more an excellent agreement between theory and simulations (Fig. 3). Minor differences might be caused by the limited resolution of our N -Body galaxy model: in particular, the potential sampling may be exceedingly poor in the outer region of the halo, where the satellites now spends a lot more time. We have tested this hypothesis performing a high resolution simulation with 10^5 particles: in this case there is a closer agreement (Fig. 3), proving the potential of the theory with respect to costly N -Body simulations.

To evaluate the decay time of a satellite moving within a singular isothermal sphere Lacey & Cole (1993) proposed the following general expression to incorporate the dependence of the sinking time on the initial eccentricity and orbital energy:

$$\tau_{DF} = T_c \epsilon^{0.78} \equiv 1.17 \frac{r_{cir}^2 V_{cir}}{GM \ln(Nm/M)} \epsilon^{0.78} \quad (15)$$

In the formula V_{cir} is the circular velocity of the satellite, r_{cir} is the radius of the circular orbit having the same energy of the actual orbit and the circularity $\epsilon \equiv J(E)/J_{cir}(E)$ is the ratio between the orbital angular momentum and that of the circular orbit having the same energy E . Lacey & Cole suggested a

value of $\alpha = 0.78$ for the dependence on eccentricity. However, as already noticed by vBLLS, the decay time τ_{DF} depends more weakly on the initial eccentricity and for the case $r_{cir}/r_t = 0.5$ vBLLS proposed a best fit of the form $\tau_{DF} \propto \varepsilon^\alpha$ whose exponent $\alpha=0.53$.

Both TLR and our N -Body simulations show that α depends on the energy of the orbit and that the value of the scale T_c deviates slightly from the one inferred using Chandrasekhar’s formula. For the cosmologically relevant orbits, the TLR approach (supported by our set of N -Body simulations), gives a $\tau_{DF} \propto \varepsilon^\alpha$ whose exponent $\alpha=0.4$.

For the case of orbits outside the halo (C98), satellites on wider orbits not only have longer decay times but the mismatch between very eccentric and nearly circular orbits becomes increasingly larger with decreasing orbital energy. A continuity in the behaviour of τ_{DF} should therefore exist when moving from peripheral orbits to internal ones. Figure 4 shows $\tau_{DF}(\varepsilon, r_{cir})$, computed using TLR, for $r_{cir}/r_t = 0.5, 0.8$, and 1. Dots refers to eccentricities $0(\varepsilon = 1)$, 0.3, 0.6, 0.8, 0.85 respectively. As mentioned in the above paragraph, the best fit gives a slope α of 0.4 for $r_{cir}/r_t = 0.5$. We find that for the typical eccentric orbits (Fig. 4) occurring in current structure formation scenarios the dynamical friction time scale is longer by a factor of 1.5-2 relative to previous estimates (Lacey & Cole 1993), a result that may affect significantly the statistics of the satellites in galaxy halos and of galaxies in galaxy clusters.

One still open problem is if orbits tend to circularize under the effect of dynamical friction. This could be true if halos lose energy faster than angular momentum. It has been recently shown (Ghigna et al. 1998) that satellites inside larger halos have a distribution of orbital eccentricities quite indistinguishable from that of the diffused dark matter component. This strongly suggests that orbits of satellites do *not* evolve significantly under the effects of tidal stripping and dynamical friction. We can now support this numerical result within TLR showing that bound orbits are not subject to any significant circularization, as illustrated in Figure 5; the result holds also when exploring the evolution of live satellites. Only when the satellite happens to fall from the very far reaches of the halo (in grazing encounters), TLR predicts some degree of circularization (C98), consistent with numerical simulations by Bontekoe & van Albada (1987).

5. The Self-Correlation Properties of the Fluctuating Microscopic Force

5.1. The Self-Correlation Time

An important results of this study is that two independent calculations, i.e., a semianalytic theory and a set of N -Body simulations give equivalent results. The quite stringent accordance between the two approaches confirm the applicability of TLR in describing the sinking of satellites in spherical nonhomogeneous halos, under the neglect of the actual stellar dynamics.

A question thus rises naturally: What is the role played by the self-gravity of the background in determining the extent of the drag ? Equation (6) contains many aspects of the self-gravity of the collisionless background (in its unperturbed state): (i) the equilibrium dynamics that establish the strength of the self-correlation properties of the system, (ii) the density profile $n_0(r)$, (iii) the virial relation that links $n_0(r)$ to the dispersion velocity $\sigma(r)$ and ultimately, (iv) the shift of the system barycenter. The braking torque depends on all these quantities that are interrelated.

The dynamics of the stars in the unperturbed potential Ψ_0 is expected to be important in the determination of \mathbf{F}_Δ if their response to the external perturbation remains correlated for a time τ^* longer than the typical radial period $T_r = 2\pi r_{cir}/V_{cir}$ (where V_{cir} is the circular velocity in the primary halo),

which is of a few time units, for the mean field potential Ψ_0 generated by the density distribution of equation (9). τ^* can be estimated using equations (3) and (4): Figure 6 shows the cumulative function

$$I^a(s) \equiv \int_{t_0}^s ds' K^a(t-s') \quad (16)$$

at four selected times ($t = 2, 3, 4, 6, 8$ time units), during orbital evolution, for $e = 0.6$ and $r_{cir} = 0.8 r_t$. We find that the rise of the correlation function K^a is rather rapid as it occurs over a time τ^* which is only $\simeq 1 T_0$, i.e., a fraction of the typical radial time T_r . On this scale τ^* , stars thus follow a dynamics that can be approximated as free: This verifies the internal consistency of our calculation and explain the equivalence between the analytical and numerical calculation.

A finite τ^* does not necessarily imply $\tau^* < T_r$. The self-correlation time scale can exceed T_r : Memory can be maintained over many orbital periods and resonant transfer of energy can accelerate dramatically the decay. As found in C98, a satellite moving outside a spherical halo experiences a drag resulting from the global tidal deformations excited by the satellite itself. The drag force was found, generally, to be

$$F_{\Delta}^a = -[GM]^2 \frac{Nm}{\sigma^2} O^{abc}(t) \int_{t_0}^t ds \mathcal{B}(t-s) Q^{bc}(s) \quad (17)$$

where the tensors Q and O represent the quadrupolar and octupolar terms leading the multipole expansion of the interaction potential (Prugniel & Combes 1992 recognized the importance of these terms in their numerical simulations). In equation (17) $\mathcal{B}(t-s)$ is a 4-point self-correlation function of the type $\langle v^x x(t-s) y y(t-s) \rangle$, gauging the degree of correlation in the equilibrium dynamics of the stars: For a purely harmonic interaction potential of proper frequency $\omega_0/2$, the function $\mathcal{B}(t-s)$ was found to scale as $\sin[\omega_0(t-s)]$. Interestingly, we here notice that for such a potential the correlation time scale is infinite. To illustrate this property, let us consider a more general expression of the self-correlation function

$$\mathcal{B}(t-s) \propto \int_{-\infty}^{+\infty} d\omega \sin(\omega(t-s)) \exp \left[-\frac{(\omega - \omega_0)^2}{\sigma_\omega^2} \right] \quad (18)$$

obtained weighting the sinusoidal function, that describes the periodic nature of the orbits of the background particles, with a Gaussian centered about ω_0 with dispersion σ_ω . We have included such a dispersion to mimic the characteristic spread in the frequencies of the background particles motions. The integral can be evaluated straightforwardly

$$\mathcal{B}(t-s) \propto \sigma_\omega \sin(\omega_0(t-s)) \exp \left[-\left(\frac{\sigma_\omega(t-s)}{2} \right)^2 \right] \quad (19)$$

to show that \mathcal{B} acquires an intrinsic cutoff time scale

$$\tau^* = 2/\sigma_\omega \quad (20)$$

which is determined by the dispersion (σ_ω) in the orbital frequencies of the equilibrium system. If the distribution is sharply peaked about $\omega_0/2$ (as for the harmonic potential) τ^* is exceedingly large and the inclusion of the actual dynamics is essential in determining the drag. As illustrated by equation (20) τ^* is finite when more frequencies are contributing to the dynamics in the virial spherical system. Hence, the “richness” in the spectral decomposition of the orbits is an indirect measure of the self-correlation time, a quantity that has to be compared with the typical radial period time T_r and with the characteristic time T_{in} of interaction (of order of T_r for the cases explored in this paper) between the satellite and the stars to determine the importance of the real dynamics in affecting the drag.

5.2. On Global Tides, the Wake and the Shift of the Barycenter

A longstanding question is whether dynamical friction in self-gravitating backgrounds is a local or global process.

As shown in C98, the satellite excites a tidal deformation when orbiting outside the halo: This deformation is clearly global as it involves the whole galaxy volume. A global response is excited also in shortlived flybys deep across the halo, giving a force along \mathbf{V} and \mathbf{R} which is proportional to the background density gradients (CP). But in addition to such a global response, a back reaction force rises due to the overdensity that the satellite excites along its path (eq. [42] and [47] of CP). This is usually referred to as being the “local” contribution to the drag depending on intensive quantities like the background density n_0 , despite the presence of a Coulomb logarithm that accounts for those “distant” encounters which are effective for the satellite’s drag. These examples (CP) illustrate that the global tidal field and the wake are aspects of the response that are simultaneously present; they can be clearly distinguished in the high velocity limit.

When considering the interaction along bound orbits inside the halo the two contributions are technically difficult to separate out. Nonetheless an approximate estimate of the degree of locality of the response can be inferred selecting from the force \mathbf{F}_Δ its component along \mathbf{V} (F_V) and comparing it with the frictional force

$$\mathbf{F}_\infty = -4\pi[GM]^2 mn_0 \ln \Lambda \left(\operatorname{erf}(x) - \frac{2x}{\pi^{1/2}} e^{-x^2} \right) \frac{\mathbf{V}}{|\mathbf{V}|} \quad (21)$$

from an infinite homogeneous non self-gravitating collisionless background (Chandrasekhar 1943; Binney & Tremaine 1987); x is equal to $|\mathbf{V}|/\sqrt{2}\sigma$.

Figure 7 shows that F_V (filled dots linked with solid line) is maximum just after each pericentric passage, the lag being a manifestation of the memory effect. F_V accounts for nearly 80 – 90% of the total force that also has a component along \mathbf{R} .

The force \mathbf{F}_∞ (dashed line) is computed using the value of the density n_0 and the dispersion velocity σ at the (“local”) instantaneous satellite’s position, and setting $\ln \Lambda = \ln(r_t/\epsilon)$ a value which is close to $\ln(Nm/M)$. In \mathbf{F}_∞ the time lag is absent, and a closer analysis of the two forces reveals that \mathbf{F}_∞ would predict a more rapid sinking than \mathbf{F}_Δ . A time dependent Coulomb logarithm can better fit the orbit and the evolution of the angular momentum, particularly in two regions: at the periphery where $\ln \Lambda \sim \ln[(r_{apo} - R(t))/\epsilon]$, and close to the halo’s center where $\ln \Lambda \sim \ln[R(t)/\epsilon]$ (see the dot-dashed line of Fig. 7). In general we find that it is difficult to reproduce accurately the evolution over a complete sample of orbits using equation (21) since the component of the force along \mathbf{R} gives a non negligible contribution: Related to the tides and to the spatial inhomogeneities, this component varies in each single path.

Customarily $\ln \Lambda$ gives indication of the interval of background particles impact parameters for which the encounter is effective. Can we have an intuitive understanding of the fits introduced above ? As guideline let us consider the temporal evolution of the density perturbation in a uniform background: Δn is found to result from the composition of disturbances that originate at earlier times s

$$\Delta n(\mathbf{r}, t) = \sqrt{\frac{2}{\pi}} GM n_0 \int_{t_0}^{t-\tau_\epsilon} \frac{ds}{\sigma^3(t-s)^2} \exp\left[-\frac{1}{2}\Gamma_s(\mathbf{R}(s) - \mathbf{r})^2\right] \quad (22)$$

which are Gaussian in space, spherically symmetric about $\mathbf{R}(s)$, and with a characteristic length

$$\lambda_s = \Gamma_s^{-1/2} = \sigma(t-s) \quad (23)$$

(In equation (22) τ_ϵ is introduced to mimic short distance encounters yielding a finite minimum impact parameter.) Since the characteristic scale length becomes increasingly small as $s \rightarrow t - \tau_\epsilon$, the deformation is large primarily in the vicinity of the satellite where $|\mathbf{R}(s) - \mathbf{r}| \ll \lambda_s$. At earlier times $s \ll t - \tau_\epsilon$ the Gaussian disturbance has a wider extension indicating that the density perturbation broadens in space and weakens in magnitude being a transient structure. (Only in the high speed limit (i.e., $\sigma/V \rightarrow 0$) the overdensity develops in a sharp edge, a shock that never broadens as stars behave as a cool continuum, i.e., as dust.) In an infinite medium the decay of the overdensity is not sufficiently rapid to make the drag finite and this is the reason why a cutoff distance, of the order of r_t , is introduced in the expression of $\ln \Lambda$ (eq. [21] is derived from eq. [6], and is a test on TLR).

In a spherical halo, the wake develops only as soon as the satellite enters the stellar medium, so the maximum impact parameter varies with time initially, as suggested by our first fitting formula. Later, the wake spatially widens while fading across the medium, in analogy with equation (22) at a rate which increases with decreasing distance r , being $\propto \sigma$ (eq. [12] and [22]). In bound nonuniform systems there is the tendency of erasing more rapidly the memory of the perturbation than in an infinite medium, yielding to a weaker drag and to a force along \mathbf{V} which is influenced more by the local properties of the background. This is likely a consequence of τ^* being smaller than the internal dynamical time. Nonetheless, the actual dynamics of the satellite can be determined only within TLR which gives the description of the full stellar response (including tides and the effect of a nonuniform background).

The coherent shift of the halo's center of mass is an important aspect of the response (White 1983; Weinberg 1989; Hernquist & Weinberg 1989; Prugniel & Combes 1992; Séguin and Dupraz 1994, 1996; Cora et al. 1997). Its inclusion accounts for the correct estimate of the global large scale density deformations induced by the satellite; pinning the center of mass of the primary (i.e., not including the shift) would result in more intense tides that instead are not excited in a real encounter. We have verified that this correction becomes important when the satellite is set on progressively wider orbits and of low eccentricity. For the vBLLS models the correction on the sinking times accounts for about 10%. It is larger $> 40\%$ when the satellite mass increases (we explored a few cases with $M/Nm = 0.08$ and $r_{cir}/r_t = 1$) and goes always in the direction of reducing the extent of the drag. Weinberg included in his formalism the shift of the barycenter of the primary system coupling the Boltzmann equation for f^{op} to the Poisson equation for the density perturbation. This approach makes the calculations too complex and does not allow for a simple expansion of the drag force in powers of the coupling constant G .

6. The Sinking of the Deformable Satellites or: How Does Tidal Stripping Affect Orbital Evolution ?

In the previous sections we have carried out a detailed study of dynamical friction using TLR and N -Body simulations to gain insight into the physical mechanisms that cause the braking of a satellite and its subsequent orbital decay. In the cases explored in §4 the satellite was treated as rigid body while real satellites are deformable systems, comprising a small luminous component hosted by a massive and extended dark matter halo.

The outer part of the dark matter halo can be strongly damaged by the tidal field of the primary, while experiencing dynamical friction. As a consequence, a reasonable picture of the evolution of satellites has to take into account the role of tidal forces as well as dynamical friction. Here we determine how mass stripping affects evolution.

Among the satellites of the Milky Way, a few have experienced at least one or two close pericenter passages and have suffered mass loss by the global tidal field of the Milky Way: a clear example is Sagittarius A which at present is in the verge of being disrupted (Ibata & Lewis 1998). Using N -Body simulations we have followed the evolution of satellites, described as spherical halos, to explore the interplay between mass stripping and orbital decay due to dynamical friction. We then tried to fit the numerical results within the framework presented in the previous sections.

6.1. Initial conditions

Large cosmological N -Body simulations within the cold dark matter (CDM) framework show that (satellite) halos have density profiles which can be fit by so called NFW or Hernquist density profiles (Navarro et al. 1996, 1997; Ghigna et al. 1998). These profiles have a central cusp and fall steeper than the isothermal profile at large radii. However, the resulting rotation curves are in conflict with those observed for dwarf galaxies and low surface brightness galaxies which exhibit a large core in the center (Moore et al. 1999a; Persic & Salucci 1997). Feedback due to mass outflows of baryons as a consequence of supernova-driven winds have been invoked to reconcile this discrepancy (Navarro et al. 1996; Gelato & Larsen 1999) but the solution of this problem still awaits (Burkert & Silk 1999). We thus employ truncated isothermal profiles with cores to model satellite halos, as these allow good fits with observed rotation curves for different galaxies (de Blok & McGaugh 1997). The primary galaxy is represented by the same model used in the simulations described in §4.

We build three different models for the satellite: these have the same virial mass M , which is $0.02Nm$, but differ in the value of the concentration c , where c is the ratio between the satellite’s tidal radius r_t^s and its core radius r_c^s . This parameter sets the value of the central density as $\rho_0 \propto c^2$. Tidal damage of satellites’ halos should be basically related to the ratio between their own central density and that of the primary halo: for this reason the concentration of the satellite’s density profile could play an important role in deciding its final fate. A general result of hierarchical clustering is that lower mass halos are on average denser because they formed earlier, when the background density of the Universe was higher. An analysis of cosmological simulations shows that the characteristic halo density scales as $M^{-\nu}$ (Syer & White 1998). The value of ν is related to the slope of the power spectrum on the scale of interest and is $\simeq 0.33$ for galaxy-sized halos in a standard CDM cosmogony: according to this estimate an LMC-like satellite should have a central density ~ 4 times higher than that of the Milky Way.

The reference model (S1) for our dark matter satellite is simply a rescaled version of the primary galaxy, according to the relations $r_t^s/r_t = (M/Nm)^{1/3}$ and $V_{cir}^s/V_{cir} = (M/Nm)^{1/3}$ (White & Frenk 1991). The resulting satellite has a circular velocity V_{cir}^s of about 50 km s^{-1} , very close to that of LMC. The other two models have a concentration which is two times (model S2) and three times (model S3) that of the reference model S1. We use 10,000 particles for the satellite models. One simulation has been rerun with 50,000 particles as a test, giving practically identical results. We employ the same system of units as in vBLS, along with the same timestep and softening for the primary system. The softening for the satellite scales as $(M/Nm)^{1/3}$ relative to the primary. We have considered only orbits with $e = 0.8$ and $e = 0.6$ for both $r_{cir}/r_t = 1$ and 0.5 . Models S2 and S3 have been run only for the most destructive encounter, i.e. for $r_{cir}/r_t = 0.5$ and $e = 0.8$.

6.2. The fate of galaxy satellites

Our results allow for a clear interpretation of the interplay between dynamical friction and mass loss due to the tidal field of the primary. Satellites lose on average about 60% of their mass after the first pericentric passage (at 1.5 Gyr), while their orbital angular momentum has decreased by no more than 20% (as illustrated in Fig. 8): this means that tidal stripping is always more efficient than dynamical friction. Their final fate however depends on their initial concentration, and, though less sensitively, on the orbital parameters. Model S1 is disrupted over a time comparable to the dynamical friction decay time τ_{DF} of its rigid counterpart, just after the second pericenter passage. (In a test with a 5×10^4 particles on a $r_{cir}/r_t = 0.5$ and $e = 0.8$ orbit, the satellite (model S1) was disrupted nearly at the same time as in the runs with 10^4 particles. This proves that the resolution used does not affect significantly the physical interpretation of our results.) Satellites with a high density contrast (S2 and S3) relative to the primary central density can instead survive even the third pericenter passage (at 5 Gyr) despite being on eccentric tightly bound orbits. They will then suffer disruption along their orbit, after 6 – 8 Gyr (performing a total of 4 – 5 pericenter passages). One has to bear in mind that these high-concentration satellites more likely correspond to the halos of small galaxies found in cosmological CDM simulations. The case of model S1 could instead represent the halo of low surface brightness satellites that typically have large cores and still have to find an explanation in a cosmological context. All satellite halos survive much longer than 10 Gyr, regardless of their concentration if they move on the peripheral orbits (with $r_{cir}/r_t = 1$). In these cases dynamical friction almost switches off, because of mass loss, when the satellite is still far from the densest region of the primary. As for the rigid case, orbital decay is not accompanied by significant circularization.

The reduced effectiveness of dynamical friction as a result of mass loss has important consequences for the merging of the baryonic components inhabiting dark matter halos. In principle, the loss of orbital angular momentum implies a decrease in the sinking time, depending on r_{cir}^2 . On the other hand the mass loss implies an increase in the sinking time, which scales as M^{-1} . The simulations have shown that substantial mass loss occurs already at the first pericentric passage, when the angular momentum has not significantly decreased yet. The satellite orbit has thus not decayed sufficiently (i.e. r_{cir} has only slightly decreased) to counterbalance the reduction in mass and the overall result is that the orbital decay will be considerably slowed down. The central region would survive the subsequent disruption of the outer dark matter halo, being more compact (Mayer et al. 1999; Navarro et al. 1995; Ghigna et al. 1998) and would then decay on a very long timescale. A decoupled orbital evolution of dark and baryonic components was already suggested by Lacey & Cole (1993) in their semianalytical treatment of galaxy merging rates. In that case it was implicitly assumed that satellites lose immediately their dark matter halos, finding themselves on a bound orbit at the periphery of the primary halo: the dynamical friction time was then computed with formula (15) adopting merely the baryonic mass for the mass of the satellite. Navarro, Frank & White (1995) instead were led to suggest that satellite galaxies merge at the center of the primary halo on a time scale determined by their initial total mass (baryonic + dark): they came up to this conclusion by directly comparing the prediction of formula (15) with the sinking times of gaseous cores in N -Body/SPH simulations of galaxy formation. Their distribution of merging times showed however a large scatter with respect to the analytical prediction: moreover, a significant group of satellites existed with sinking times 2 – 3 times larger than the analytical estimate. This turned out to be satellites with an initial mass $< 1/10$ of their primary halo, i.e. they were in the mass range of typical galaxy satellites. Our results suggest the higher efficiency of tidal stripping with respect to dynamical friction is responsible for such an increase of merging times of galaxy satellites.

We can now give an estimate of the merging time that incorporates mass loss as well as orbital decay.

We can approximate the mass loss curve obtained for satellites moving on eccentric tightly bound orbits (which are the most likely for satellites) with an exponentially decreasing function of time given by:

$$M(t) = M_d \exp(-t/T_r) + M_b \quad (24)$$

where M_d is the dark mass of the satellite, corresponding roughly to its initial total mass, M_b is the baryonic mass, which we assume to be $< 1/10$ of the total mass, and T_r is the orbital radial period. The satellites continue to lose mass at every pericenter passage: however, most of their mass is stripped already on the first orbit and this occurs independently of their concentration. Moreover, at this time the orbital parameters are still very close to the initial ones due to the low efficiency of the orbital decay. We then use the tidally limited mass at the first pericentric passage (M_d/e) as the “effective” mass for the satellite in formula (15). The merging time of the satellite galaxies τ_m can be then computed using

$$\tau_m = 1.2 \frac{J_{cir} r_{cir}}{[GM_d/e] \ln(M_{halo}/M_d)} \epsilon^{0.4} \quad (25)$$

where J_{cir} and r_{cir} are, respectively, the initial orbital angular momentum and radius of the circular orbit with the same energy of the orbit on which the satellite is placed. This formula updates the one by Lacey & Cole incorporating both the different normalization factor and eccentricity dependence as well as the “delaying” effect due to tidal stripping. The reliability of this prescription was tested by running a simulation with a rigid satellite on an orbit $e = 0.8$ with an initial mass reduced by a factor $(1/e)$ with respect to the standard mass and then comparing the angular momentum loss in this case with that occurring in the corresponding run with the deformable satellite (Fig. 9). These are remarkably close, while much more angular momentum is lost by the rigid satellite with the standard mass, which suffers complete orbital decay (Fig. 9). Our estimate suggest that the satellite galaxies would merge on a timescale almost 2 – 3 times larger than previously estimated with (15). In addition, our N -Body simulations indicate that the survival time t_s of the dark matter halos of the satellites falls between τ_{DF} and τ_m , with more concentrated haloes surviving for a longer time. However, the presence of a baryonic core inside the halo can prolong the lifetime of the central part of the halo itself because the overall potential well becomes deeper (Mayer et al. 1999). Only very large satellites (i.e. satellites with a mass $> 1/10$ relative to that of the primary) could decay on a short timescale compared to the Hubble time, as the rate of orbital angular momentum loss would be comparable to the rate of mass loss (this being related only to the ratio of the central densities of the two systems and not to their masses). Such events could have occurred in the building up of our galaxy, at $z > 1$ when the progenitor halo at that time probably accreted big lumps on orbits with small pericenters (because the virial radius of the primary was smaller), a condition which should further reduce dynamical friction time scale (see also Kravtsov & Klypin 1998). Satellites accreted after that epoch had not enough time to decay and merge and these are the present-day satellites of the Milky Way and Andromeda.

7. Discussion and Conclusion

In this paper we present, for the first time, a unified view of the physical process responsible for the braking of a satellite in a self-gravitating spherical stellar system. We have shown that TLR embraces all aspects of the gravitational interaction of a massive object with a background of lighter (dark matter) self-gravitating particles.

We have found that the characteristic dynamical friction time for satellites with mass ratios < 0.1 (moving on cosmologically relevant orbits) in a galaxy like our Milky Way is sufficiently long that satellites

have not merged with the stellar disk yet. As first noticed by Ghigna et al. (1998), orbital decay is not followed by a significant circularization when the satellite happens to orbit well inside the primary halo. The expected equilibrium distribution of eccentricities in a spherical potential is skewed toward high $e \simeq 0.6 - 0.7$ (see vBLLS) and dynamical friction plays no role in modifying such a distribution. We have in addition shown that rigid satellites on eccentric orbits have sinking times only slightly shorter than those of satellites on circular orbits: previous analysis instead predicted a wider spread, implying a much shorter lifetime in the primary halo. Tidal stripping is more efficient than dynamical friction for the typical masses of galaxy satellites. We have shown that this should considerably prolong the lifetime of the baryonic lumps inhabiting satellite halos with masses up to 0.1 that of the primary halo, so that they will wander along their orbit for at least an Hubble time. This has important implications for many issues concerning the evolution of galaxies. We indeed expect that those satellites that entered the primary halo after $z \sim 1$ cannot have decayed to the center yet, while their dark matter halo has been already substantially stripped. These correspond to the present-day satellites of spiral galaxies, like those populating our Local Group.

Our results show that the disk is unlikely to have suffered any late merging event or penetrating encounter with a typical satellite. The overall picture which emerges is that substructure survives longer than previously believed and this nicely agrees with numerical findings in large cosmological simulations (Ghigna et al. 1998; Tormen et al. 1998; Klypin et al. 1999). In general, the pericenters of the orbits of satellites are reduced by no more than a factor of 2 in about 7 Gyr, which is approximately the time which passes between $z = 1$ and $z = 0$. This large population of almost indestructible satellites could have a dramatic effect on the dynamics of spiral galaxies disks. Work by Moore et al. (1999b) suggests that the cumulative effect of many nearby encounters between this numerous population of small satellites on almost radial orbits and a galactic disk would heat its stellar component considerably on a time scale of a few Gyrs even without merging with it.

Dynamical friction and tidal stripping are among the main dynamical mechanisms involved during the formation of cosmic structures. Our results provide a detailed description of these processes as well as giving the theoretical support for understanding much of the underlying physics. Numerical simulations and theoretical models are now converging towards a common picture where CDM models create a large wealth of long lived substructure in dark matter halos. It now remains to investigate its effects and its observational evidence, so providing tight constraints on theories of galaxy formation and evolution.

We thank J. Binney for enlightening discussion and T. Quinn and J. Stadel for kindly providing the PKDGRAV code. This work acknowledges financial support from MURST.

APPENDIX

In this Appendix we shortly describe the semianalytical calculation for the drag force $\mathbf{F}_\Delta(t)$ acting on the satellite at time t (eq. [6]). The Force is computed under the hypothesis expressed in equation (8) considering a Gaussian distribution function in the velocity space for which $\nabla_{\mathbf{v}} f^{\text{op}} = -(\mathbf{v}/\sigma^2)f^{\text{op}}$. Due to the complexity of the various expressions we introduce the vector

$$\mathbf{X} \equiv \mathbf{R}(t) - \mathbf{r}, \tag{A1}$$

and define

$$\nabla_{\mathbf{R}(s)}\tilde{\phi} \equiv \nabla_{\mathbf{R}(s)}\phi(|\mathbf{R}(s) - \mathbf{r}|) - \int d_3\mathbf{r}' n_0(r') \nabla_{\mathbf{R}(s)}\phi(|\mathbf{R}(s) - \mathbf{r}'|). \quad (\text{A2})$$

The integral on the velocity space can be written in a simplified form, so the force reads

$$F_{\Delta}^b(t) = -[GM]^2 Nm \left(\frac{1}{2\pi} \right)^{3/2} \int_{t_0}^t \frac{ds}{(t-s)^4} \int d_3\mathbf{r} \frac{n_0(r)}{\sigma^5(r)} \frac{\partial \tilde{\phi}}{\partial R^a(s)} \frac{\partial I^a}{\partial R^b(t)} \quad (\text{A3})$$

where the vector \mathbf{I} is found to have components

$$I^a = \frac{2\pi}{\Gamma} \frac{X^a}{\mathbf{X}} \int_0^{+\infty} dy y \phi(y) \times$$

$$\left\{ (X^2 - Xy + \Gamma^{-1}) \exp[-\frac{1}{2}\Gamma(X-y)^2] - (X^2 + Xy + \Gamma^{-1}) \exp[-\frac{1}{2}\Gamma(X+y)^2] \right\} \quad (\text{A4})$$

with $\Gamma \equiv [\sigma(t-s)]^{-2}$. Since \mathbf{I} can be expressed as gradient of a scalar function we are able to determine the force as

$$F_{\Delta}^b(t) = [GM]^2 Nm \left(\frac{1}{2\pi} \right)^{1/2} \int_{t_0}^t ds \int d_3\mathbf{r} \frac{n_0(r)}{\sigma(r)} \frac{\partial \tilde{\phi}}{\partial R^a(s)} \times$$

$$\frac{\partial^2}{\partial R^b(t) \partial R^a(t)} \frac{1}{|\mathbf{R}(t) - \mathbf{r}|} \int_0^{+\infty} dy y \phi(y) \left\{ \exp[-\frac{1}{2}\Gamma(X-y)^2] - \exp[-\frac{1}{2}\Gamma(X+y)^2] \right\} \quad (\text{A5})$$

Equation (A5) involves integrals over the physical volume of the halo, over time s and y . The integral in the y variable can be computed analytically, given the expression of the potential $\phi(y)$. According to our analysis of §3, the function ϕ is just the spline kernel potential ϕ_{sp} introduced by Hernquist & Katz (1989; we refer to his Appendix) that reduces to the Newtonian potential ($\phi = -1/y$) at distances larger than 2ϵ : this potential is written as an expansion in powers of y . In equation (A5) we thus need to calculate integrals of the form

$$\int_{inf}^{sup} dy y^n \left\{ \exp[-\frac{1}{2}\Gamma(X-y)^2] - \exp[-\frac{1}{2}\Gamma(X+y)^2] \right\} \quad (\text{A6})$$

with $n \geq 0$; the domain of integration (inf, sup) is uniquely defined by the form of ϕ_{sp} . If we introduce the functions

$$B_n(a, \Gamma) \equiv B_n(a, X, \Gamma) - B_n(a, -X, \Gamma) \quad (\text{A7})$$

with

$$B_n(a, X, \Gamma) \equiv \int_0^a dy y^n \exp[-\frac{1}{2}\Gamma(X+y)^2] \quad (\text{A8})$$

and

$$B_n(a, -X, \Gamma) \equiv \int_0^a dy y^n \exp[-\frac{1}{2}\Gamma(y-X)^2] \quad (\text{A9})$$

we can express $B_n(a, \Gamma)$ as a linear combination of Error Functions, and the following recurrence relations apply:

$$B_0(a, X, \Gamma) = \left(\frac{\pi}{2\Gamma} \right)^{1/2} \left\{ \text{erf}[\sqrt{(\Gamma/2)}(X+a)] - \text{erf}[\sqrt{(\Gamma/2)}X] \right\} \quad (\text{A10})$$

$$B_1(a, X, \Gamma) = -XB_0(a, X, \Gamma) - \frac{1}{\Gamma} \left\{ \exp[-\frac{\Gamma}{2}(X+a)^2] - \exp[-\frac{\Gamma}{2}X^2] \right\} \quad (\text{A11})$$

$$B_{n+1}(a, X, \Gamma) = -XB_n(a, X, \Gamma) + \frac{n}{\Gamma}B_{n-1}(a, X, \Gamma) - \frac{a^n}{\Gamma} \exp[-\frac{\Gamma}{2}(X+a)^2]. \quad (A12)$$

The integral on the y variable in equation (A5) is constructed using equations (A6-A12).

Given the above relations we can calculate also the first and second derivatives of B , B' and B'' , relative to X ; after a number of simple but long steps we can express the drag force as

$$F_{\Delta}^b = -[GM]^2 Nm \left(\frac{1}{2\pi} \right)^{1/2} \int d_3\mathbf{r} \frac{n_0(r)}{\sigma} \times \int ds \nabla_{\mathbf{R}(s)}^a \tilde{\phi} \left\{ \left[\frac{3X^a X^b}{X^5} - \frac{\delta^{ab}}{X^3} \right] \sum_n c_n [B_n([d], \Gamma) - XB'_n([d], \Gamma)] + \frac{X^a X^b}{X^3} \sum_n c_n B''_n([d], \Gamma) \right\} \quad (A13)$$

where $B_n([d], \Gamma)$ shortly denotes that the functions of equations (A6-A9) are computed over the whole domain $(0, \infty)$ which is divided into three parts $(0, \epsilon)$, $(\epsilon, 2\epsilon)$ and $(2\epsilon, +\infty)$ (see Hernquist & Katz 1989). The coefficient c_n in equation (A13) contains the n th power of the softening length ϵ , as shown in the expression of ϕ_{sp} . The time and spatial integrals are computed numerically, using standard procedures, given the density and velocity dispersion profiles (eq. [9] and [12]).

REFERENCES

- Bekenstein, J.D., & Maoz, E. 1992, ApJ, 390, 79
- Binney, J., & Tremaine, S. 1987, Galactic Dynamics, Princeton Univ. Press
- Bontekoe, Tj.R., & van Albada, T.S. 1987, MNRAS, 224,349
- Burkert, A., & Silk, J. 1999, astro-ph/9904159
- Chandrasekhar, S. 1943, ApJ, 97, 255
- Colpi, M., & Pallavicini, A. 1998, ApJ, 502, 150 (CP98)
- Cora, S.A., Muzzio, J.A., & Vergne, M.M. 1997, MNRAS, 289, 253
- Colpi, M. 1998, ApJ, 502, 167 (C98)
- De Blok, W.J.G., & McGaugh, S.S. 1997, MNRAS, 290,533
- Dikaiakos, M., & Stadel, J. 1996, ICS Conference Proceedings 1996
- Gelato, S., & Sommer-Larsen, J. 1999, MNRAS, 303, 321
- Ghigna, S., Moore, B., Governato, F., Lake, G., Quinn, T., & Stadel, J. 1998, MNRAS, 300, 146
- Hernquist, L., & Weinberg, M.D. 1989, MNRAS, 238, 407
- Hernquist, L., & Katz, N. 1989, ApJS, 70, 419
- Hernquist, L. 1993, ApJS, 86, 389
- Kravtsov, A.V., & Klypin, A.A. 1998, astro-ph/9812311
- Klypin, A.A., Kravtsov, A.V., Valenzuela, O., & Prada, F. 1999, astro-ph/9901240
- Kandrup, H.E. 1981, ApJ, 244, 316

- Ibata, R.A., & Lewis, G.F. 1998, *ApJ*, 500, 575
- Lacey, C., & Cole, S. 1993, *MNRAS*, 262, 627
- Mayer, L., Governato, F., Colpi, M., Moore, B., Quinn, T.R., & Baugh, C.M. 1999, *astro-ph/9903442*
- Mayer, L., Governato, F., Colpi, M., Moore, B., Quinn, T.R., & Baugh, C.M. 1999, in preparation
- Moore, B., Quinn, T., Governato, F., Stadel J., & Lake, G. 1999a, *astro-ph* 9903164
- Moore, B., Governato, F., Lake, G., Stadel, J., & Quinn T.R. 1999b, submitted to *apj*
- Navarro, J.F., Frenk, C.S., & White, S.D.M. 1995, *MNRAS*, 275, 56
- Navarro, J.F., Eke, V.R., & Frenk, C.S. 1996, *MNRAS*, 283, L72
- Navarro, J.F., Frenk, C.S., & White, S.D.M. 1997 *MNRAS*, 490, 493
- Nelson, R.W., & Tremaine, S. 1997, *astro-ph/9707161*
- Persic M. & Salucci P., 1997, in "Dark and visible matter in galaxies", ASP Conference, 117 ed. M.Persic
P.Salucci
- Prugniel, P., & Combes, F. 1992, *A&A*, 259, 25
- Séguin, P., & Dupraz, C. 1996, *A&A*, 310, 757
- Séguin, P., & Dupraz, C. 1994, *A&A*, 290, 709
- Syer, D., & White, S.D.M. 1998, *MNRAS*, 29, 337
- Stadel, J., & Quinn, T.R. 1998, in preparation
- Tormen, G., Diaferio, A., Syer, D. 1998, *MNRAS*, 299, 728
- Weinberg, M.D., 1986, *ApJ*, 300, 93
- Weinberg, M.D., 1989, *MNRAS*, 239, 549
- White, S.D.M. 1983, *ApJ*, 274, 53
- White, S.D.M., & Frenk, C.S. 1991, *ApJ*, 379, 25
- van den Bosch, F.C., Lewis, G.F., Lake, G., & Stadel, J. 1999, *astro-ph/9811229*, to appear in *ApJ*

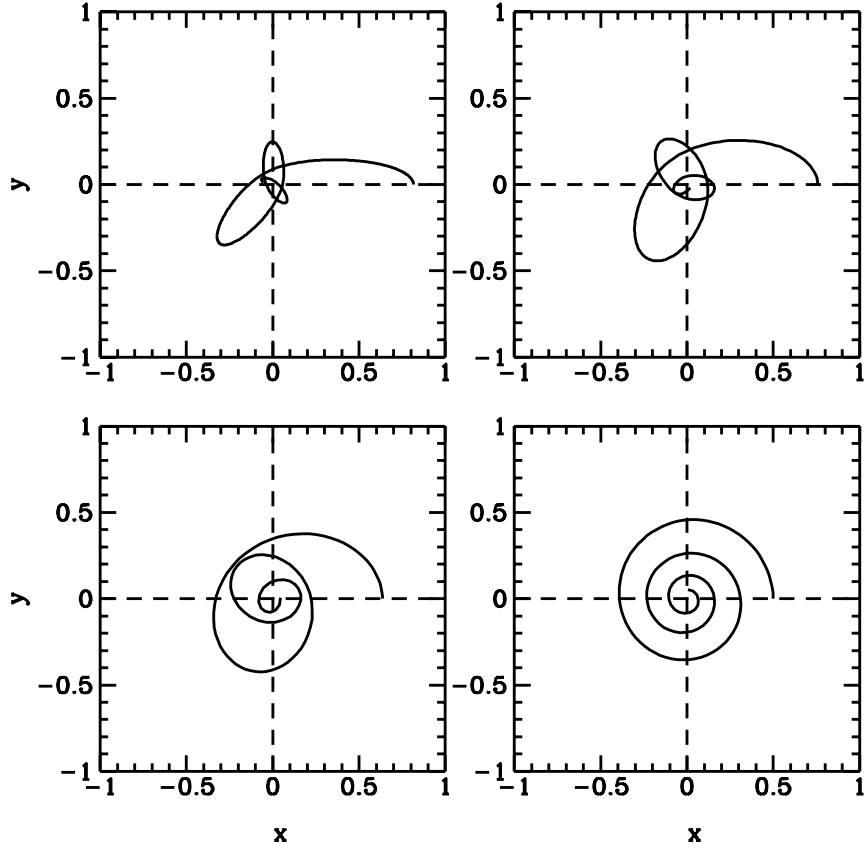


Fig. 1.— Collection of orbits in the plane (x, y) computed within TLR, for $r_{cir}/r_t = 0.5$. From top left to bottom right the initial eccentricity is $e = 0.8, 0.6, 0.3, 0$, respectively. Length is in units of r_t .

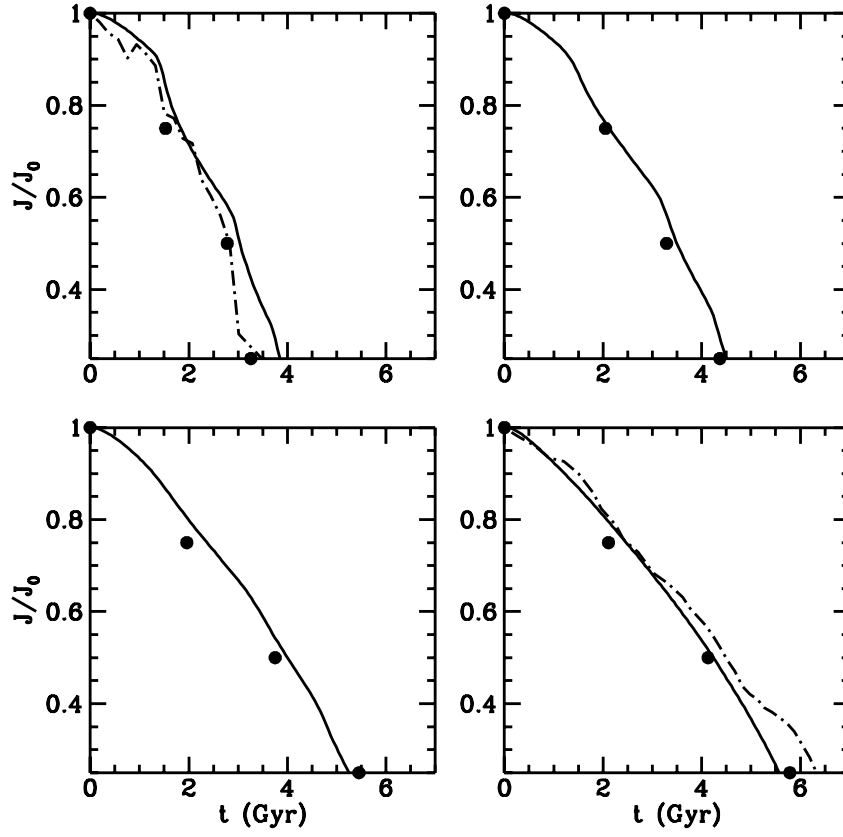


Fig. 2.— Orbital angular momentum J (in units of the initial value J_0) as a function of time for $r_{cir}/r_t = 0.5$. From top left to bottom right the eccentricity e is 0.8, 0.6, 0.3, 0. Solid lines indicate the results of TLR, filled circles are the results of vBLLS, and dot-dashed lines are the results of our N -Body runs.

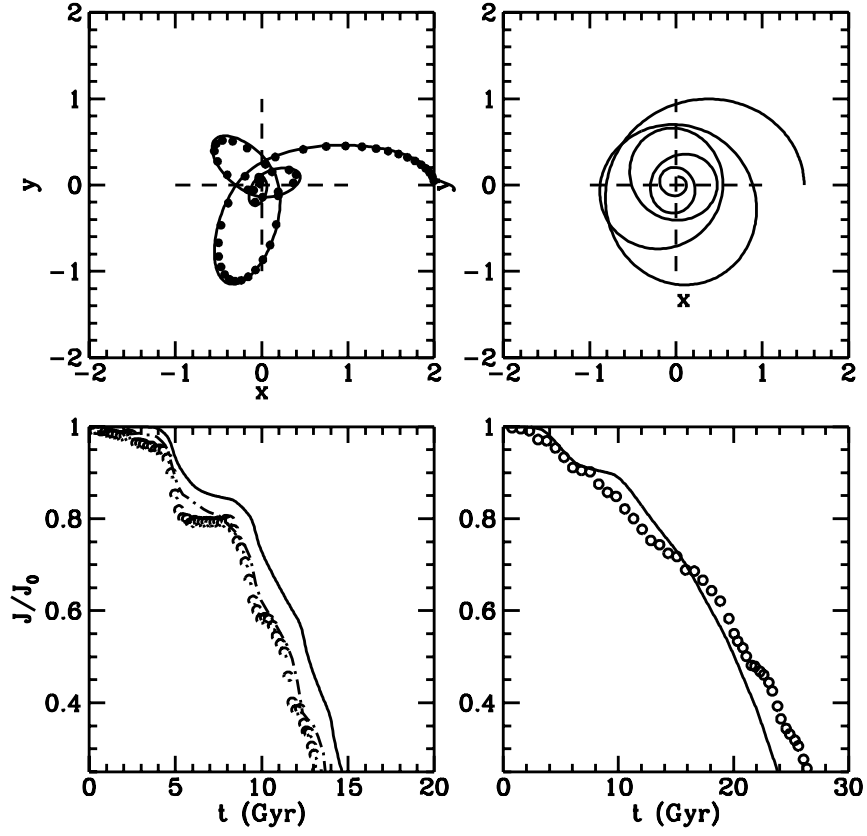


Fig. 3.— In the upper panel we show the satellite’s orbital evolution computed within TLR (solid line) for $r_{cir}/r_t = 1$ for $e = 0.8$ (left) and $e = 0.3$ (right). Filled circles are from our N -Body simulation using 100,000 particles. In the lower panel we report the corresponding evolution of J/J_0 . The dot-dashed line in the lower left panel is the result of the simulation with 100,000 particles. Open dots are from the N -Body runs with 20,000 particles. Length are in units of r_t , and time is in Gyr corresponding to 1.34 time units.

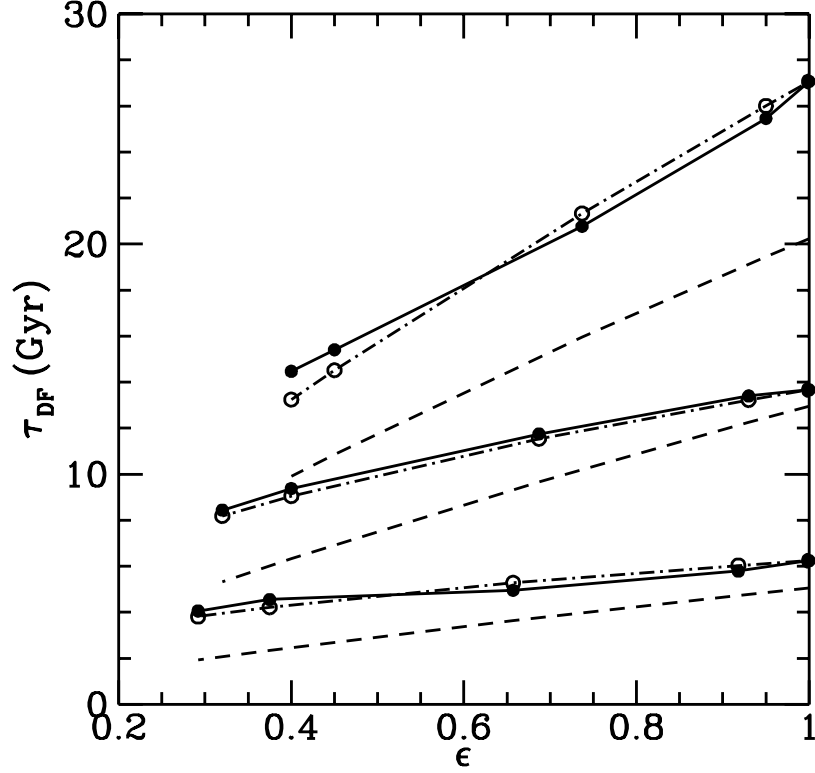


Fig. 4.— Dynamical friction time scale τ_{DF} (in Gyr) against circularity $\epsilon = J/J_{cir}$. τ_{DF} refers to the time at which $J/J_0 = 0.01$. Filled Dots connected with solid line denote the decay times computed within TLR, for $r_{cir}/r_t = 0.5$ (bottom curve), 0.8 (mid curve) and 1 (top curve). Open circles (connected with dot-dashed line) are the fit with $\alpha = 0.4$ (bottom), $\alpha = 0.45$ (mid) and $\alpha = 0.78$ (top). The dashed line denotes the fitting formula by Lacey & Cole, given by eq. [15].

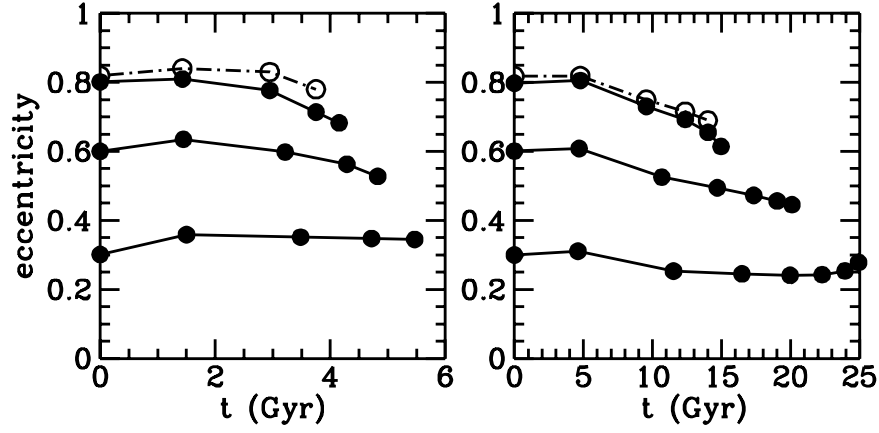


Fig. 5.— Eccentricity as a function of time t , for r_{cir}/r_t equal to 0.5 (left panel) and 1 (right panel), and initial $e = 0.8, 0.6, 0.3$. Filled dots are from TLR while the open dots are from the N -Body runs. Eccentricity is computed at each pericentric passage considering a complete cycle along the actual satellite’s orbit.

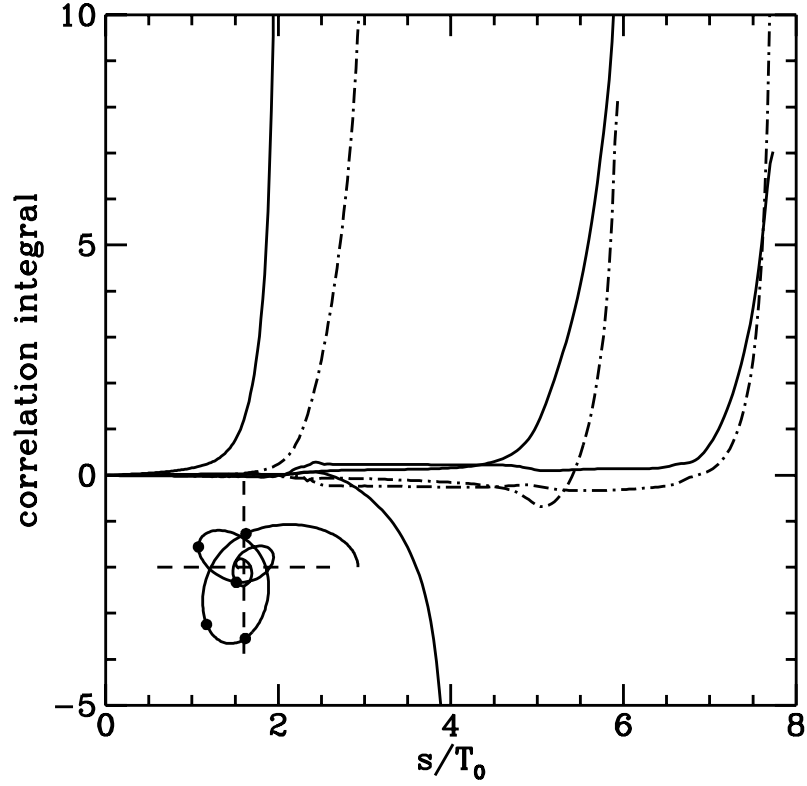


Fig. 6.— The correlation integrals $I^x(s)$ (solid line) and $I^y(s)$ (dot-dashed line) as defined in eq. [16] with s varying from $t_0 = 0$ up to t with time in dimensionless units. A view of the orbit (with $r_{cir}/r_t = 0.8$ and $e = 0.6$) in the (x, y) plane is drawn, where dots denote the times t/T_0 equal to 2,3,4,6,8 at which the functions I (proportional to the components of the drag force and expressed in dimensionless units) are computed.

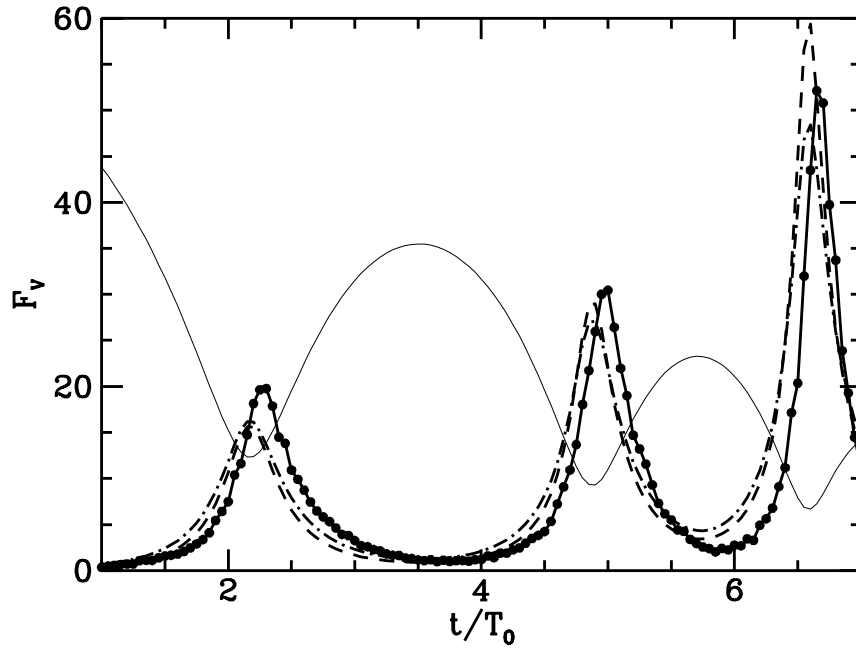


Fig. 7.— Filled circles connected with solid line denote the component of \mathbf{F}_Δ along \mathbf{V} (in arbitrary units) as a function of the dimensionless time. The dashed line is \mathbf{F}_∞ evaluated for $\ln \Lambda = \ln(r_t/\epsilon)$ while the dot-dashed line gives \mathbf{F}_∞ for $\ln \Lambda = \ln(R(t)/\epsilon)$. In the background (lighter solid line on an arbitrary scale) we have drawn the current satellite distance $R(t)$ relative to the stellar center of mass.

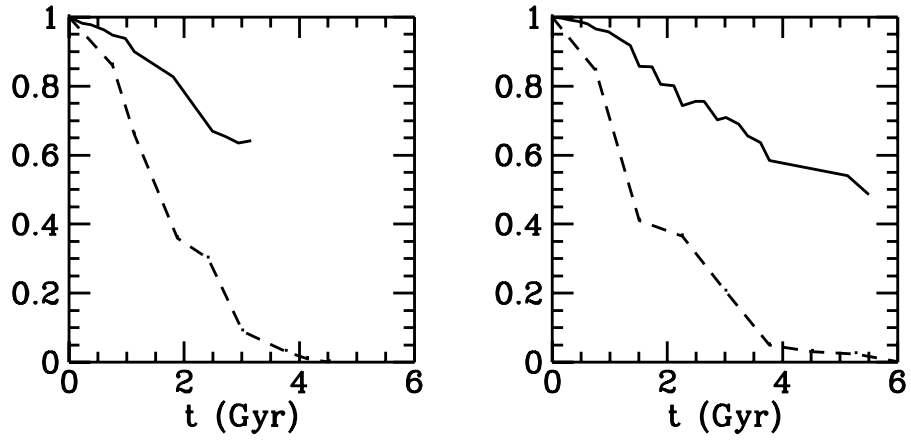


Fig. 8.— Comparison between mass loss (dashed line) and orbital angular momentum loss (solid line) as a function of time, for model S1 and $r_{cir}/r_t = 0.5$. The left panel refers to an orbit with $e = 0.8$, the right is for $e = 0.6$

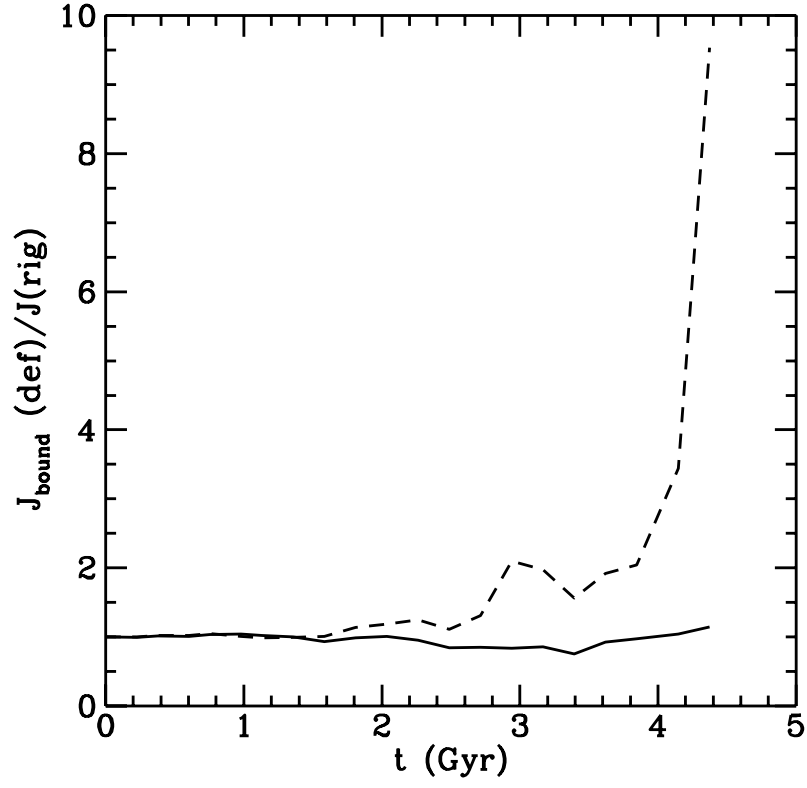


Fig. 9.— Ratio of $J(t)/J_0$ for the bound matter of the deformable S2 satellite with $J(t)/J_0$ for the rigid satellite. Curves are for $r_{cir} = 0.5$ and eccentricity equal to 0.8. Dashed line refers to a rigid satellite with M equal to the initial mass of the deformable satellite. Solid line refers to a rigid satellite with mass reduced by the e-folding factor ($1/e$).